Climate and density-dependent population dynamics: Lessons from a simple high-Arctic ecosystem

Running title: Climate and density-dependent dynamics

Submitted as a *Letter*

Dominique Fauteux[1] (dfauteux@nature.ca), Audun Stien[2] (audun.stien@uit.no), Nigel G. Yoccoz[2] (nigel.yoccoz@uit.no), Eva Fuglei[3] (eva.fuglei@npolar.no), Rolf A. Ims[2] (rolf.ims@uit.no)

[1]Canadian Museum of Nature, Centre for Northern Studies, Gatineau (QC) Canada.

[2]Department of Arctic and Marine Biology, UiT The Arctic University of Norway, Tromsø, Norway.

[3]Norwegian Polar Institute, Tromsø, Norway

Statement of authorship

DF wrote the first complete draft of the manuscript and conducted CMR analyses; AS collected data in the field, conducted population modelling, and contributed substantially to revisions; NGY, EF and RAI collected data and contributed substantially to revisions.

Data accessibility

All data used in this work will be deposited in a public repository (i.e. Dryad) upon request or publication.

Number of words: Abstract, 151 words; Main text, 4 278 words

Number of references: 71

Number of tables: 1

Number of figures: 5

Corresponding author:

Dominique Fauteux

1740, chemin Pink, Gatineau (QC) J9H 6Y8, Canada

Abstract

The strikingly diverse population dynamics of herbivorous small mammals, ranging from high-amplitude, multi-annual cycles to relatively stable dynamics, have puzzled ecologists for a century. Theory predicts that this diversity is shaped by density-dependent food web interactions and stochastic weather events. Recent disrupted cycles through amplitude dampening have been attributed to climate change. However, empirical testing has been hampered by the complexity of the food webs in which these herbivores normally are found. Here we analyze population dynamics of a grazing vole species in a uniquely simple high-Arctic food web without top-down regulation. In accordance with theory, the population dynamics was mostly ruled by overcompensatory density-dependence in winter that without environmental stochasticity would have yielded seasonality driven high-amplitude 2-year cycles. In this simple food web, rain-on-snow events disrupted cyclicity, but not through amplitude dampening. Our case study highlights how food web structure may modify the impact of climate change on population dynamics.

Introduction

Theory suggests that contrasting population dynamics result from details in the pattern of density-dependence, including its strength and shape, whether it acts instantly or with a delay, and how it interacts with deterministic (seasonal) and stochastic (weather) components of the prevailing or changing climate (Royama 1992; Stenseth 1999; Bjørnstad & Grenfell 2001; May 2001; Turchin 2003). Studies of small rodents have contributed much to elucidating the different facets of density-dependent and density-independent population dynamics (Stenseth 1999; Turchin 2003). A central topic has been what sort of density dependence yields the high-amplitude, multi-annual population cycles - for which voles and lemmings have become so renowned (Elton 1942; Finnerty 1981; Stenseth & Ims 1993; Krebs 2013). Based on time series analyses, delayed-density dependence is reckoned as a main determinant of population cycles (see Stenseth 1999 and Barraquand *et al.* 2017 for reviews), although overcompensatory direct density dependence appears to be an alternative in some settings (Barraquand *et al.* 2014). As rodent cycles are most prevalent in northern ecosystems with profound climatic seasonality (Elton 1942; Ims & Fuglei 2005; Krebs 2013; but see Korpimäki *et al.* 2005; Lambin *et al.* 2006), several studies have emphasised that annual density dependence ought to be decomposed into its seasonal components (Hansen *et al.* 1999a; Stenseth *et al.* 2003; Cornulier *et al.* 2013) - both to accurately account for the density-dependent structure that underlies the observed dynamics and to identify the season-specific biotic mechanisms that cause density dependence. Considering seasonal dynamics is also crucial to assess the role of climatic stochasticity, because such external forcing differs between summer and winter (Cornulier *et al.* 2013; Korpela *et al.* 2013). The role of climate forcing is now also accentuated by the recent collapses and

dampening of population cycles in several ecosystems that appear to be associated with ongoing climate change (Ims *et al.* 2008; Gilg *et al.* 2009; Cornulier *et al.* 2013).

Linking density dependence to the biotic mechanisms that causally generate the diversity of population dynamics patterns in small mammals have proved to be challenging. Most rodent populations are imbedded in complex food webs, and hence, subjected to a multitude of biotic interactions that could cause the different facets of density-dependent population growth. For instance, delayed and direct density dependence may result from several trophic interactions as well as intrinsic population mechanisms (Hansen *et al.* 1999b; Barraquand *et al.* 2014; Myers 2018). While field experiments have helped pinpointing some mechanisms (Ostfeld *et al.* 1993; Ims & Andreassen 2000; Graham & Lambin 2002; Huitu *et al.* 2003; Fauteux *et al.* 2016), they have been too short-term to be conclusive with respect to what generate different patterns of multi-annual population dynamics.

Here we apply an approach that has proved useful for unravelling the effects of density dependence and climatic stochasticity in herbivorous large mammals (e.g. Grenfell *et al.* 1998; Coulson *et al.* 2001; Hansen *et al.* 2019), namely to target populations that are found in very simple biotic settings. Hence, our study targets a high-arctic population of the graminivorous (grass-eating) East European vole (*Microtus levis*) in a food web that lack biotic interactions (i.e. predation) that cause complex density dependence in most other small mammal populations. By combining statistical analyses of long-term, high-quality live-trapping data with simulations of a population model parameterized from these data, we (1) test theoretical conjectures about what sort of density dependence and resultant population dynamics is expected to emerge in such a simple biotic setting and (2) assess how climatic stochasticity impinge on such density dependent population dynamics. Finally, we point out how the insights from our case study shed new light

on the longstanding puzzle about what generate population cycles and how ongoing climate change may influence these cycles.

Methods

Study population

Our study is located by Grumant in Svalbard (78.18°N, 15.13°E). This high Arctic location is characterised by cool summers (July average: 5.9°C) and cold winters (January average -16.2°C) with little precipitation (average 190 mm, period 1960-1990; Førland *et al.* 1997). Average daily air temperatures at the nearby weather station (Longyearbyen airport, 13 km away), are typically above 0°C in early-to-mid June - September. Winter temperatures are much more variable than summer temperatures (Yoccoz & Ims 1999), with standard deviations of monthly mean temperatures being 5.1°C for February and 0.9°C for July. In winter, temperature extremes can vary between -44°C and 6°C, while in summer they vary between 0°C and 21°C (Førland *et al.* 1997). Rain-on-snow (ROS) events is a relatively frequent, stochastically occurring phenomenon in Svalbard (Hansen *et al.* 2019) - calculated as the sum of precipitation at temperature above 1°C in the winter months November-April. ROS range from approximately 0 to 66 mm per year and is most prevalent at the beginning of the winter period (November-January; Stien *et al.* 2012). ROS events have been found to strongly influence the population dynamics of all year-round resident vertebrate populations in Svalbard (Hansen *et al.* 2013).

The East European vole belongs to one of the most speciose and widespread genera (*Microtus*) of small mammals with presence in temperate, boreal and Arctic biomes (Tamarin 1985). Most *Microtus* species are graminivorous (i.e. grass-eating) and have multivoltine life histories (e.g. multiple generation per year). The East European vole was accidentally introduced

in Svalbard in the first half of the 20th century (Fredga *et al.* 1990). The voles still have a highly restricted distribution and are found in coastal slopes of bird cliffs in association with seabird fertilized tundra vegetation dominated by graminoids, particularly Polar foxtail *Alopecurus ovatus* (Elvebakk 1994). The best habitats have soils and lush grass vegetation on the top of boulders that provide food, drainage and shelter for the fossorial voles.

There are no other small mammals present in Svalbard, which suggests virtually no interspecific competition (Koivisto *et al.* 2007). The Arctic fox (*Vulpes lagopus*) is the only terrestrial predator present, but acts as a generalist carnivore that mostly rely on seabirds in the study area (Frafjord 2002). East European voles reproduce quickly with females observed to be gravid as early as 17 days old (Yoccoz *et al.* 1993) and may live at high population densities (>100 ind. ha^{-1}; Koivisto *et al.* 2007). The population dynamics of many *Microtus* voles have been studied extensively on the European continent where they typically exhibit 3-4-yr multi-annual cycles (Korpimäki *et al.* 2005; Lambin *et al.* 2006; Cornulier *et al.* 2013; Barraquand *et al.* 2014).

Live trapping

East European voles were live-trapped during the years 1990-2007. Here, we analysed two data sets. The main data set used for analysis of seasonal density dependence and demography was obtained from one of the largest and lushest vole habitat patches in Svalbard; hereafter termed Core area (Fig. 1). From 1990 to 1996, we used a trapping grid of 93 Ugglan Special multiple-capture traps encompassing 4.5 ha of the Core area, while from 2002-2006 the grid was made of 74 traps and encompassed 2.8 ha. Traps were separated by approximately 20 m and placed by burrow entrances wherever possible. Trapping of the Core area followed the robust design of

Pollock (1982) and consisted of three primary periods (late June/early July [hereafter termed July] = P1; early August = P2; and early September = P3), each with 6 to 10 secondary periods, except in 1990 when primary periods spanned only the first half of the summer. We used a second, more long-term data set for assessing the annual population dynamics obtained from a linear habitat on a ridge and vegetated part of the ravine at the western edge of the Core area (hereafter termed Ridge; Fig. 1). The Ridge area was monitored with 30 traps in August during 1991-2007, with the same number of secondary periods as for the Core area. Oats and potatoes were used as baits in the morning (07h00) and traps were checked twice during the day (13h00 and 19h00). Traps were deactivated during the last trapping period of the day. Captured voles were marked by toe clipping, sexed and weighed. The study was conducted according to the regulations for research in Svalbard during the study period.

Density estimation

The densities of the vole population in the Core and Ridge areas was derived by spatially-explicit capture-recapture (SECR) models with the package *secr* in R (Efford 2020; R Core Team 2020). Briefly, these models have the advantage of estimating capture probabilities based on the distance separating the center of activities of an individual from a trap (Borchers & Efford 2008). By using a two-parameter (i.e. probability of capture at the center of activities and a measure of home range size) half-normal detection function, we obtained more accurate estimates of the area effectively surveyed (Krebs *et al.* 2011). For the Core area, we used one null SECR model per trapping period per year with the Huggins parameterisation to estimate density (Krebs *et al.* 2011). For the Ridge area, annual densities were obtained for the August trapping period only. Densities of male and female adults (body mass ≥25 g) and sub-adults (body mass <25 g;

Yoccoz *et al.* 1993) were derived from this general model. Because the movement of voles in Svalbard is restricted by habitat, we used a 20 m buffer around traps to build the state-space that is used to estimate effective sampling area. The Nelder-Mead algorithm was used for optimisation of the likelihood in model fitting.

Annual density-dependent structure and temporal variability

We used the annual early August SECR density estimates from the Ridge area to assess the density-dependent structure. We modelled ln-transformed densities from the 17-year time series using a second-order autoregressive model (Stenseth 1999; Turchin 2003). Coefficients obtained from this type of model inform about direct ($\beta_{t\text{-}1}$) and delayed density-dependence ($\beta_{t\text{-}2}$), and may also be interpreted with respect to the presence of cyclic dynamics and cycle periods (Royama 1992). We observed zero vole densities in the Ridge area in 1996 and 2002 and the time series was modelled using $\log(D_t + \Delta)$ with $\Delta = 1$. A range of values for Δ, from $\Delta = 0.2$ to $\Delta = 2$, were investigated, but the choice of Δ was not found to affect parameter estimates and conclusions substantially. We used the standard deviation of the log10 transformed time series as a metric for the temporal variability (i.e. the amplitude) of the multiannual dynamics (*s*-index; Stenseth & Framstad 1980). The *s*-index has been used both to define cyclic dynamics (index values > 0.5; Henttonen *et al.* 1985) and to compare populations across environmental gradients (Hansson & Henttonen 1985, 1988; Ehrich *et al.* 2020).

Seasonal density dependence and climate effects on population growth

We used the following model to explore patterns of variation in population growth in summer and winter in the Core area:

$$X_{t+1} = X_t * e^{r_t * \Delta t} \quad (1)$$

Where X_t is the true population density at time *t*, r_t is the population growth rate from t to t+1 and Δt is the time period from *t* to *t*+1 (in months). Furthermore, we modelled r_t as a linear function of X_t, climatic stochasticity in winter (C_t, i.e. ROS) and residual stochastic variation in *r* (process error, ε_t):

$$r_t = \beta_0 + \beta_X * X_t + \beta_C * C_t + \varepsilon_t \quad (2)$$

where we assume that process error $\varepsilon_t \sim N(0, \sigma_r^2)$ and β_0, β_X, β_C and σ_r^2 are parameters estimated by the data. Measurement error was included in the model assuming a log normal distribution for the densities estimated using the SERC model, D_t, giving:

$$D_t \sim \text{lnorm}(\log_e(X_t), \sigma_{D,t}^2) \quad (3)$$

The log normal measurement error standard deviation, $\sigma_{D,t+1}$, was estimated using estimates of the standard error of D_t (SE(D_t)) obtained in the SECR analysis:

$$\sigma_{D,t} = \log_e((SE(D_t) / D_t)^2 + 1) \quad (4)$$

The model (equations 1-3) was fitted in JAGS version 4.2.0 (Plummer 2003). Point estimates of r_t and associated 95 % credibility intervals presented in figures were obtained by

fitting a model for r_t (equation 2) with time fitted as a factor, i.e. $r_t = \beta_t$. In addition to parameter estimates and associated 95% credibility intervals we report estimates of Bayesian R^2 for the models (Gelman *et al.* 2019). The Bayesian R^2 was estimated as the mean of R_i^2 = var(fit$_i$) / (var(fit$_i$) + var(residuals$_i$)), where i index the update number in the MCMC simulation, var(fit$_i$) = var($\beta_{0,i} + \beta_{X,i} * X_t + \beta_{C,i} * C_t$) and var(residuals$_i$) = $\sigma_{r,i}^2$.

Analyses of population growth were done separately for the approximately 2.5 month summer period (June/July-September) and for the approximately 9.5 month winter period (September-June/July) as we expected the population dynamics to differ substantially in these two seasons. In the winter we expected the amount of ROS to have effects on population growth (Stien *et al.* 2012; Hansen *et al.* 2013).

Summer population growth could be estimated from the change in densities from June/July (t) to August (t + 1) and from August (t + 1) to September (t + 2). Differences between these periods were investigated by fitting period as a factor in the model for population growth (equation 2). Population growth rates were not estimated for the summer of 1996, when there were no voles captured in the study area, and 2002, when there were no voles captured in the first and second primary trapping periods and an estimate of 1 vole per hectare (3 voles caught) in the third primary period. The very low density estimates in September 2002 and the absence of voles in 1996 implied adoption of methodological adjustments, that are detailed in supplementary material, to allow growth rate estimates over the associated winters.

The timing of the primary trapping periods differed somewhat in 1990-1991 from subsequent years. In 1990, all the trapping was early in the season and the time period from primary period 1 to primary period 3 was only 0.7 months. We therefore only used data from primary period 1 and 3 to estimate population growth, to get a time period that was more similar

to the other years (Δt = 1.2-1.7 months). In 1991 it was only 2 weeks between primary period 1 and 2 and we used only estimates from primary period 2 and 3 in the analyses.

Model simulations of multiannual population dynamics

We simulated the annual population dynamics linking summer and winter population growth from:

$$X_{a,t+1} = X_{s,t} * e^{r_{s,t} * \Delta t_s} \quad (5)$$

$$X_{s,t+1} = X_{a,t} * e^{r_{w,t} * \Delta t_w} \quad (6)$$

where $X_{s,t}$ and $X_{a,t}$ is population density in the spring and autumn in year *t* respectively, $r_{s,t}$ and $r_{w,t}$ are population growth rates (month^{-1}) in summer and winter respectively, and Δt_s and Δt_w are the time periods of the summer and winter seasons respectively ($\Delta t_s + \Delta t_w = 12$).

Using equation (2), $r_{j,t}$ were modelled with parameters estimated from the data (Table 2). Our baseline deterministic model included only density dependence ($r_{j,t} = \beta_{j,0} + \beta_{j,X} * X_{j,t}$) and assumed 3 months of summer and 9 months of winter. The sensitivity of population dynamics to changes in parameter values were evaluated using bifurcation diagrams and analyses of autocorrelation.

Demography

The demographic structure of the population was analysed using SECR based estimates of subadult and adult, male and female vole densities. Recruitment was determined by comparing

densities of subadults to adult female densities. We analysed densities of male and female voles within age categories to detect sex differences.

Survival and maturation rates of subadult and adult, male and female voles were estimated using multi-events models implemented in the software E-Surge (Choquet *et al.* 2009). For the summer estimates were obtained for the periods of July-August and August-September. The data did not allow demographic rates for the winter period (September-July) to be estimated, because too few individuals captured in year t survived the winter and were recaptured year t+1. The maturation rate is the probability of a subadult to develop into the adult stage from one primary period to the next. Survival, maturation and detection probabilities were modelled as functions of covariates using a logit link function. Year, period (July-August vs. August-September) and sex were considered as covariates for all demographic rates. In addition, age (subadults vs. adults) was considered in models for survival and detection rates. Furthermore, we evaluated the effect of vole density, D_t, as an environmental covariate in models of survival and maturation rates. Model selection was based on Akaike information criterion corrected for overdispersion (QAICc; Anderson *et al.* 1994) and estimates used in the model simulations (see below) were retained from the model judged most parsimonious model using AICc.

The effect of density on survival and maturation was first determined by whether the covariate was significant in the most parsimonious, non-temporal model. If yes, we tested if the variance explained by the covariate was significant by using an ANODEV with M_t being the most parsimonious temporal model, M_c as being the most parsimonious model with density as a covariate (possibly with an interaction density*time), and M_0 as the model without density or time as a covariate (Grosbois *et al.* 2008).

Results

Annual population dynamics

The 1991-2007 time series of annual estimates of Eastern European vole densities from the Ridge trapping area was characterised by high amplitude population fluctuations with 2 - 4 years between subsequent crash years (Fig. 1). The population dynamics appeared to be stationary; i.e. there were no evidence for temporal trends in mean or variance in densities over the 17 years. The amplitude of the fluctuations (s-index=0.57) was within the range found in population time series of cyclic Arctic lemming populations (Ehrich *et al.* 2020). However, in contrast to most other Arctic populations, first (r = -0.39) and second-order (r = 0.02) autocorrelation coefficients showed no evidence of cyclic dynamics.

A second-order autoregressive model supported only direct density dependence ($\beta_{t\text{-}1}$ = -0.46, 95% confidence interval [CI]: [-0.70, 0.02]), while delayed density dependence was estimated to be close to zero ($\beta_{t\text{-}2}$= -0.15, 95% CI: [-0.65, 0.34]). These estimates suggest population dynamics with dampened 2-year cycles (Royama 1992), and that sustained fluctuations were upheld by the high unstructured error variance (σ^2 = 1.3).

Seasonal density dependence

The analysis of the seasonal population density estimates from the Core trapping area during 1990-1996 and 2002-2006 (cross-correlation of vole densities with the Ridge trapping area, r = 0.92; Fig. 1), showed that the summer population growth rates were all positive (Fig. 2 and 3a). This suggests that the vole population densities remained below carrying capacity. Still, there were evidence for density dependence in that population growth rates were negatively related to density in the previous month (Table 1, Fig. 3a).

297 In contrast, winter population growth rates were negative in many of the years. The
298 negative population growth rates in winter were associated with both high vole densities in the
299 previous autumn and high levels of ROS in the winter (Table 1, Fig. 3b). Overall, the data
300 suggest strong population regulation from direct density-dependence in the winter period.
301
302 *Simulated population dynamics*
303 A deterministic version of a seasonal density-dependent model fitted to the data would generate
304 stable 2-year vole cycles. These 2-yr cycles were relatively robust to changes in climate severity
305 in winter, in that high ROS have to become the norm for a change to stable dynamics with a
306 single equilibrium density (Fig. 4a). The 2-yr cycle in the baseline model was also robust to
307 changes in season lengths as climate change would have to reduce the winter length to well
308 below 8 months for more complex dynamics to appear (Fig. 4b). However, the signal of the 2-yr
309 cycles deteriorated fast with increasing levels of stochastic process error (Fig. 4c). At the
310 observed levels of process error the expected second order autocorrelation was close to zero in
311 the model simulations ($r = 0.02$); i.e. similar to what was estimated from the time series data.
312 Finally, temporal variability as quantified by the s-index increased with increasing process error
313 (Fig. 4d).
314
315 *Demography*
316 Sub-adult male and female voles occurred at similar densities, with no evidence for a systematic
317 deviance from a 1:1 sex ratio (Fig. 5a). The sex ratio of adults approached a 2:1 female-bias at
318 high female densities (Fig. 5b). This pattern was consistent with strong density-dependent
319 regulation of adult male densities in summer, with growth rates close to zero at ~14 adult male

voles ha^{-1} (Fig. 5c). There was no strong evidence for adult female population growth to be density-dependent (β_D = -0.015, CI=[-0.034, 0.005]). Recruitment in the population remained also relatively stable across densities with a ratio of sub-adults to adult females being close to 1:1 (Fig. 5d).

Both survival and maturation rates varied significantly between years as well as among demographic categories (sex and age) and summer periods (Supplementary material, Table S1, Fig. S1) in a manner that contributed to the high process error in the summer population growth (Table 1). Survival rate was density-dependent, and stronger in females than in males (Supplementary material, Table S2, Fig. S2), whereas there was no evidence for density-dependence in maturation rates (Supplementary material, Table S2, Fig. S3).

Discussion

Without significant top-down regulation from predators, the focal study system is essentially reduced to a simple two-link food chain consisting of a multivoltine herbivore population and their graminoid food plants in a profoundly seasonal environment. Here we have presented the first empirical analysis of such an ecological system that so far only has been subjected to theoretical investigations. Such systems have been modelled mechanistically in continuous time to identify under which circumstances multiannual herbivore population cycles can be expected (Oksanen 1990; Turchin & Batzli 2001). Moreover, theoreticians have thoroughly investigated the dynamical properties of phenomenological discrete-time models with seasonal direct density-dependence (Kot & Schaffer 1984), akin to the model we here parameterized with field data. The core insight from this theory - and indeed also our empirical study - is that the profound seasonality destabilises the dynamics of such simple systems (White & Hastings 2020). Profound

seasonality in terms of a long arctic winter without primary production implies that carrying capacity in summer greatly exceeds that of the winter. Such environmental setting combined with a multivoltine life history and a weakly density-dependent summer growth rate allows the herbivore population to overshoot its winter carrying capacity, and thus induce violent population crashes due to overcompensatory direct density dependence.

Interestingly, the continuous-time, plant-herbivore model analysed by Turchin and Batzli (2001) with a graminoid-type plant regrowth function, multivoltine herbivore population dynamics and high-arctic seasonality without stochasticity, generated 2-year cycles like our baseline model. We are not aware that such short population cycles have ever been observed in any mammal populations. Neither are we aware of any other cases of such high-amplitude, high-frequency boom-bust vole population dynamics without a clear cyclic signal as we observed in our high-arctic study system. In multivoltine rodents, cycle lengths typically vary between 3-5 years in ecosystems with profound seasonality, while non-cyclic populations often seen in environments with less pronounced seasonality have such low-amplitude fluctuations that they are termed stable (Hansson & Henttonen 1988; Bjørnstad *et al.* 1995). It is commonly assumed that any cycle generating mechanism must induce delayed density dependence (Stenseth 1999; Ims & Fuglei 2005; Barraquand *et al.* 2017; Myers 2018), although opinions differ about which mechanisms are in place (Turchin *et al.* 2000; Gauthier *et al.* 2009). Seasonality is in itself a source of delay in producer-consumer interactions (Oksanen 1990), but is expected to yield only 2-year cycles if the delay is less than a year. The rapid regrowth of graminoids (Turchin & Batzli 2001) – even after high vole peak densities and severe winter grazing (Klemola *et al.* 2000) – prevents the one-year delay that generates the longer cycles often found in graminivorous voles. We also notice that the lack of delayed density dependence in our study system does not support

366 that delays due to intrinsic mechanisms such as stress-induced maternal effects (Boonstra *et al.*
367 1998) were influential. In fact, the only demographic feature that could be attributed to intrinsic
368 regulation was adult sex ratio, which became more female biased with increasing population
369 density - as could be expected from the polygynous mating system of graminivorous voles (Ims
370 1987). Finally, our study supports previous studies proposing that the action of the almost
371 ubiquitous guild of specialist rodent predators in boreal and Arctic food webs normally cause the
372 delayed density dependence that was lacking in our study system (Hanski *et al.* 1993; Turchin *et*
373 *al.* 2000; Gilg *et al.* 2003). Indeed, the absence of specialist rodent predators in high-Arctic
374 Svalbard is the most likely cause of the exceptional vole population dynamics observed here.
375 Experimental predator removals (Ims & Andreassen 2000; Klemola *et al.* 2000; Fauteux *et al.*
376 2016) have never been conducted at sufficient spatial and temporal scale to investigate the
377 outcome on multiannual population dynamics.

378 A fundamental question in population ecology accentuated by global climate change is
379 how abiotic environmental variation can modify the effect of density-dependent biotic
380 interactions. Our study adds to previous studies showing that episodes of mild winter weather in
381 boreal and Arctic ecosystems may lead to population crashes in herbivores (Aars & Ims 2002;
382 Korslund & Steen 2006; Dominé *et al.* 2018) and disrupt population cycles (Ims *et al.* 2008;
383 Kausrud *et al.* 2008; Gilg *et al.* 2009; Korpela *et al.* 2013). Previous models has shown that
384 climatically disrupted population cycles in multivoltine rodents readily collapses to low-
385 amplitude fluctuations and hence stable populations dynamics in presence of both direct and
386 delayed density dependence (Ims *et al.* 2008; Kausrud *et al.* 2008; Gilg *et al.* 2009). Here we
387 have shown that population cycles in a simpler trophic system with only direct density-
388 dependence may also easily be disrupted by increasing climatic stochasticity, however, without

any dampening effect on the dynamics. Hence, our case study provides support to the general conjecture that the impact of climate change on ecological systems is dependent on their structure and hence can be expected to be diverse across time and space (Coulson *et al.* 2001; Gilg *et al.* 2009; Korpela *et al.* 2013).

Acknowledgements

The following institutions financed the fieldwork in Svalbard: Research Council of Norway, Governor of Svalbard, Nansen Endowment, French Polar Institute, and French Embassy of Norway. The present study, which is a contribution from the Climate-ecological Observatory for Arctic Tundra (COAT), was funded by Svalbard Environmental Protection Fund. The following people contributed to the trapping of voles during the 18 summers in Svalbard: Harald Steen, Jon Aars, Ottar N. Bjørnstad, Thomas Hansteen, Christophe Pelabon, Siw T. Killengreen, Edda Johannesen, Harry P. Andreassen, Gry Gundersen, Thor Aasberg and Xavier Lambin.

References

Aars, J. & Ims, R.A. (2002). Intrinsic and climatic determinants of population demography: the winter dynamics of tundra voles. *Ecology*, 83, 3449-3456.

Anderson, D.R., Burnham, K.P. & White, G.C. (1994). AIC model selection in overdispersed capture-recapture data. *Ecology*, 75, 1780-1793.

Barraquand, F., Louca, S., Abbott, K.C., Cobbold, C.A., Cordoleani, F., DeAngelis, D.L. *et al.* (2017). Moving forward in circles: challenges and opportunities in modelling population cycles. *Ecol. Lett.*, 20, 1074-1092.

411 Barraquand, F., Pinot, A., Yoccoz, N.G. & Bretagnolle, V. (2014). Overcompensation and phase
412 effects in a cyclic common vole population: between first and second-order cycles. *J.*
413 *Anim. Ecol.*, 83, 1367-1378.
414 Bjørnstad, O.N., Falck, W. & Stenseth, N.C. (1995). Geographic gradient in small rodent
415 density-fluctuations - a statistical modeling approach. *Proc. R. Soc. B-Biol. Sci.*, 262,
416 127-133.
417 Bjørnstad, O.N. & Grenfell, B.T. (2001). Noisy clockwork: time series analysis of population
418 fluctuations in animals. *Science*, 293, 638-643.
419 Boonstra, R., Krebs, C.J. & Stenseth, N.C. (1998). Population cycles in small mammals: the
420 problem of explaining the low phase. *Ecology*, 79, 1479-1488.
421 Borchers, D.L. & Efford, M.G. (2008). Spatially explicit maximum likelihood methods for
422 capture–recapture studies. *Biometrics*, 64, 377-385.
423 Choquet, R., Rouan, L. & Pradel, R. (2009). Program E-Surge: a software application for fitting
424 multievent models. In: *Modeling Demographic Processes In Marked Populations* (eds.
425 Thomson, DL, Cooch, EG & Conroy, MJ). Springer US Boston, MA, pp. 845-865.
426 Cornulier, T., Yoccoz, N.G., Bretagnolle, V., Brommer, J.E., Butet, A., Ecke, F. *et al.* (2013).
427 Europe-wide dampening of population cycles in keystone herbivores. *Science*, 340, 63-
428 66.
429 Coulson, T., Catchpole, E.A., Albon, S.D., Morgan, B.J.T., Pemberton, J.M., Clutton-Brock,
430 T.H. *et al.* (2001). Age, sex, density, winter weather, and population crashes in Soay
431 sheep. *Science*, 292, 1528-1531.

Dominé, F., Gauthier, G., Vionnet, V., Fauteux, D., Dumont, M. & Barrere, M. (2018). Snow physical properties may be a significant determinant of lemming population dynamics in the high Arctic. *Arct. Sci.*, 4, 813-826.

Efford, M.G. (2020). secr: spatially explicit capture-recapture models. R package version 4.2.0. http://CRAN.R-project.org/package=secr.

Ehrich, D., Schmidt, N.M., Gauthier, G., Alisauskas, R., Angerbjörn, A., Clark, K. *et al.* (2020). Documenting lemming population change in the Arctic: Can we detect trends? *Ambio*, 49, 786-800.

Elton, C.S. (1942). *Voles, mice and lemmings. Problems in population dynamics.* Clarendon press, Oxford.

Elvebakk, A. (1994). A survey of plant associations and alliances from Svalbard. *Journal of Vegetation Science*, 5, 791-802.

Fauteux, D., Gauthier, G. & Berteaux, D. (2016). Top-down limitation of lemmings revealed by experimental reduction of predators. *Ecology*, 97, 3231-3241.

Finnerty, J.P. (1981). *The population ecology of cycles in small mammals*. Yale University Press, New Haven.

Førland, E.J., Hanssen-Bauer, I. & Nordli, P.Ø. (1997). *Climate statistics and longterm series of temperature and precipitation at Svalbard and Jan Mayen*. Norwegian Meteorological Institute, Oslo.

Frafjord, K. (2002). Predation on an introduced vole *Microtus rossiaemeridionalis* by arctic fox *Alopex lagopus* on Svalbard. *Wild. Biol.*, 8, 41-47.

453 Fredga, K., Jaarola, M., Anker Ims, R., Steen, H. & G. Yoccoz, N. (1990). The 'common vole' in
454 Svalbard identified as *Microtus epiroticus* by chromosome analysis. *Polar Res.*, 8, 283-
455 290.
456 Gauthier, G., Berteaux, D., Krebs, C.J. & Reid, D. (2009). Arctic lemmings are not simply food
457 limited - a comment on Oksanen et al. *Evol. Ecol. Res.*, 11, 483-484.
458 Gelman, A., Goodrich, B., Gabry, J. & Vehtari, A. (2019). R-squared for Bayesian regression
459 models. *Am. Stat.*, 73, 307-309.
460 Gilg, O., Hanski, I. & Sittler, B. (2003). Cyclic dynamics in a simple vertebrate predator-prey
461 community. *Science*, 302, 866-868.
462 Gilg, O., Sittler, B. & Hanski, I. (2009). Climate change and cyclic predator–prey population
463 dynamics in the high Arctic. *Global Change Biol.*, 15, 2634-2652.
464 Graham, I.M. & Lambin, X. (2002). The impact of weasel predation on cyclic field-vole
465 survival: the specialist predator hypothesis contradicted. *J. Anim. Ecol.*, 71, 946-956.
466 Grenfell, B.T., Wilson, K., Finkenstädt, B.F., Coulson, T.N., Murray, S., Albon, S.D. *et al.*
467 (1998). Noise and determinism in synchronized sheep dynamics. *Nature*, 394, 674-677.
468 Grosbois, V., Gimenez, O., Gaillard, J.-M., Pradel, R., Barbraud, C., Clobert, J. *et al.* (2008).
469 Assessing the impact of climate variation on survival in vertebrate populations. *Biol.*
470 *Rev.*, 83, 357-399.
471 Hansen, B.B., Gamelon, M., Albon, S.D., Lee, A.M., Stien, A., Irvine, R.J. *et al.* (2019). More
472 frequent extreme climate events stabilize reindeer population dynamics. *Nat. Commun.*,
473 10, 1616.

474 Hansen, B.B., Grøtan, V., Aanes, R., Sæther, B.-E., Stien, A., Fuglei, E. *et al.* (2013). Climate
475 events synchronize the dynamics of a resident vertebrate community in the High Arctic.
476 *Science*, 339, 313-315.
477 Hansen, T.F., Stenseth, N.C. & Henttonen, H. (1999a). Multiannual vole cycles and population
478 regulation during long winters: an analysis of seasonal density dependence. *Am. Nat.*,
479 154, 129-139.
480 Hansen, T.F., Stenseth, N.C., Henttonen, H. & Tast, J. (1999b). Interspecific and intraspecific
481 competition as causes of direct and delayed density dependence in a fluctuating vole
482 population. *Proc. Natl. Acad. Sci.*, 96, 986-991.
483 Hanski, I., Turchin, P., Korpimäki, E. & Henttonen, H. (1993). Population oscillations of boreal
484 rodents: regulation by mustelid predators leads to chaos. *Nature*, 364, 232-235.
485 Hansson, L. & Henttonen, H. (1985). Gradients in density variations of small rodents: the
486 importance of latitude and snow cover. *Oecologia*, 67, 394-402.
487 Hansson, L. & Henttonen, H. (1988). Rodent dynamics as community processes. *Trends Ecol.*
488 *Evol.*, 3, 195-200.
489 Henttonen, H., McGuire, A.D. & Hansson, L. (1985). Comparisons of amplitudes and
490 frequencies (spectral analyses) of density variations in long-term data sets of
491 *Clethrionomys* species. *Ann. Zool. Fenn.*, 22, 221-227.
492 Huitu, O., Koivula, M., Korpimäki, E., Klemola, T. & Norrdahl, K. (2003). Winter food supply
493 limits growth of northern vole populations in the absence of predation. *Ecology*, 84,
494 2108-2118.
495 Ims, R.A. (1987). Male spacing systems in microtine rodents. *Am. Nat.*, 130, 475-484.

496 Ims, R.A. & Andreassen, H.P. (2000). Spatial synchronization of vole population dynamics by
497 predatory birds. *Nature*, 408, 194-196.
498 Ims, R.A. & Fuglei, E. (2005). Trophic interaction cycles in tundra ecosystems and the impact of
499 climate change. *Bioscience*, 55, 311-322.
500 Ims, R.A., Henden, J.A. & Killengreen, S.T. (2008). Collapsing population cycles. *Trends Ecol.*
501 *Evol.*, 23, 79-86.
502 Kausrud, K.L., Mysterud, A., Steen, H., Vik, J.O., Ostbye, E., Cazelles, B. *et al.* (2008). Linking
503 climate change to lemming cycles. *Nature*, 456, 93-U93.
504 Klemola, T., Koivula, M., Korpimäki, E. & Norrdahl, K. (2000). Experimental tests of predation
505 and food hypotheses for population cycles of voles. *Proc. R. Soc. B-Biol. Sci.*, 267, 351-
506 356.
507 Koivisto, E., Huitu, O. & Korpimäki, E. (2007). Smaller *Microtus* vole species competitively
508 superior in the absence of predators. *Oikos*, 116, 156-162.
509 Korpela, K., Delgado, M., Henttonen, H., Korpimäki, E., Koskela, E., Ovaskainen, O. *et al.*
510 (2013). Nonlinear effects of climate on boreal rodent dynamics: mild winters do not
511 negate high-amplitude cycles. *Global Change Biol.*, 19, 697-710.
512 Korpimäki, E., Oksanen, L., Oksanen, T., Klemola, T., Norrdahl, K. & Banks, P.B. (2005). Vole
513 cycles and predation in temperate and boreal zones of Europe. *J. Anim. Ecol.*, 74, 1150-
514 1159.
515 Korslund, L. & Steen, H. (2006). Small rodent winter survival: snow conditions limit access to
516 food resources. *J. Anim. Ecol.*, 75, 156-166.
517 Kot, M. & Schaffer, W.M. (1984). The effects of seasonality on discrete models of population
518 growth. *Theor. Popul. Biol.*, 26, 340-360.

519 Krebs, C.J. (2013). *Population fluctuations in rodents*. The University of Chicago Press,
520 Chicago.
521 Krebs, C.J., Boonstra, R., Gilbert, S., Reid, D., Kenney, A.J. & Hofer, E.J. (2011). Density
522 estimation for small mammals from livetrapping grids: rodents in northern Canada. *J.*
523 *Mammal.*, 92, 974-981.
524 Lambin, X., Bretagnolle, V. & Yoccoz, N.G. (2006). Vole population cycles in northern and
525 southern Europe: Is there a need for different explanations for single pattern? *J. Anim.*
526 *Ecol.*, 75, 340-349.
527 May, R.M. (2001). *Stability and complexity in model ecosystems*. Printeton University Press,
528 Princeton, New Jersey.
529 Myers, J.H. (2018). Population cycles: generalities, exceptions and remaining mysteries. *Proc. R.*
530 *Soc. B-Biol. Sci.*, 285, 20172841.
531 Stenseth, N.C. & Framstad, E. (1980). Reproductive effort and optimal reproductive rates in
532 small rodents. *Oikos*, 34, 23-34.
533 Oksanen, L. (1990). Exploitation ecosystems in seasonal environments. *Oikos*, 57, 14-24.
534 Ostfeld, R.S., Canham, C.D. & Pugh, S.R. (1993). Intrinsic density-dependent regulation of vole
535 populations. *Nature*, 366, 259-261.
536 Plummer, M. (2003). JAGS: A program for analysis of Bayesian graphical models using Gibbs
537 sampling. In: *Proceedings of the 3rd International Workshop on Distributed Statistical*
538 *Computing* Vienna, Austria.
539 Pollock, K.H. (1982). A capture-recapture design robust to unequal probability of capture. *J.*
540 *Wildl. Manag.*, 46, 752-757.

R Core Team (2020). R: A language and environment for statistical computing. R Foundation for Statistical Computing, Vienna, Austria. Available at: http://www.R-project.org/.

Royama, T. (1992). *Analytical population dynamics*. Chapman and Hall.

Stenseth, N.C. (1999). Population cycles in voles and lemmings: density dependence and phase dependence in a stochastic world. *Oikos*, 87, 427-461.

Stenseth, N.C. & Ims, R.A. (1993). *The biology of lemmings*. Academic press, London.

Stenseth, N.C., Viljugrein, H., Saitoh, T., Hansen, T.F., Kittilsen, M.O., Bølviken, E. *et al.* (2003). Seasonality, density dependence, and population cycles in Hokkaido voles. *Proc. Natl. Acad. Sci.*, 100, 11478-11483.

Stien, A., Ims, R.A., Albon, S.D., Fuglei, E., Irvine, R.J., Ropstad, E. *et al.* (2012). Congruent responses to weather variability in high arctic herbivores. *Biol. Lett.*, 8, 1002-1005.

Tamarin, R.H. (1985). *Biology of new world Microtus*. American Society of Mammalogists, United-States.

Turchin, P. (2003). *Complex population dynamics*. Princeton University Press, Princeton, New Jersey.

Turchin, P. & Batzli, G.O. (2001). Availability of food and the population dynamics of arvicoline rodents. *Ecology*, 82, 1521-1534.

Turchin, P., Oksanen, L., Ekerholm, P., Oksanen, T. & Henttonen, H. (2000). Are lemmings prey or predators? *Nature*, 405, 562-565.

White, E. R., and A. Hastings. 2020. Seasonality in ecology: Progress and prospects in theory. *Ecol. Complex.*, 44, 100867.

Yoccoz, N.G. & Ims, R.A. (1999). Demography of small mammals in cold regions: the importance of environmental variability. *Ecol. Bull.*, 47, 137-144.

564 Yoccoz, N.G., Ims, R.A. & Steen, H. (1993). Growth and reproduction in island and mainland
565 populations of the vole Microtus epiroticus. *Can. J. Zool.*, 71, 2518-2527.

566

Tables

Table 1. Parameter estimates for the best models for monthly population growth of Eastern European voles (equations 1-5) over winter and in the summer period and estimates of the Bayesian R^2 for the models. No rain-on-snow (ROS) effect was included in the model for summer population growth, giving no estimate of β_{ROS}.

	Winter		Summer	
Parameter	mean	95 % C. I.	mean	95 % C. I.
β_0	0.23	(0.14, 0.33)	0.64	(0.44, 0.83)
β_D	-0.0040	(-0.0058, -0.0024)	-0.0051	(-0.0095, -0.0006)
β_{ROS}	-0.0043	(-0.0074, -0.0014)	-	-
σ_r^2	0.005	(0.001, 0.020)	0.020	(0.005, 0.058)
Bayesian R^2	0.92	(0.73, 0.98)	0.40	(0.02, 0.76)

β_0 = intercept; β_D = coefficient for density at time *t*; β_{ROS} = coefficient for effect of ROS; σ_r^2 = process error variance.

Figure legends

Figure 1. Picture of the Core and Ridge areas for live-trapping East European voles near Grumantbyen on Svalbard (**a**) and time series of vole densities (**b**) estimated in August in the Core area (gray shape, lines points, years 1990-1996 and 2002-2006) and the Ridge area (black shape, lines and points, years 1991-2007). Error bars represent 95% confidence intervals.

Figure 2. Population density of the East European vole in the Core area near the Grumant area in Svalbard (lines and points) and precipitations of rain on snow during the previous winter (Rain-on-snow; black bars in **a** only). The total population densities are shown in **a**. In **b**, adult males (solid blue circles and lines), adult females (solid red squares and lines), subadult males (open pale blue circles and lines), and subadult females (open pale red squares and lines) are shown. Densities were obtained using spatially-explicit capture-recapture models with the Huggins parameterisation. Dotted lines indicate change in population size during winter. The thin grey bands indicate winter when trapping was not conducted. The wide grey band between 1996 and 2002 indicate no trapping during that period. Error bars represent 95% confidence intervals. Notice the difference in scale between **a** and **b**. In 1990, trapping periods were in early July, late July, and mid-August. In 1991, trapping periods were early July, late July, and mid-September, whereas for all other years trapping was done in the first part of each month.

Figure 3. Estimated monthly population growth rates (r) in summer in relation to population density in month *m* (**a**) and monthly winter population growth rate in relation with population density in year *t* measured in September (**b**) of East European voles. In **a**, filled points represent the early summer period (July-August) and open points the late summer period (August-

September) each year. In **b**, the points represent average monthly growth over the period September-July and point size reflect the amount of rain-on-snow (ROS, mm) that fell during the winter. Error bars represent 95% confidence and credibility intervals along respectively the x and y - axis. Parameter estimates for the regression lines (with 95% C.I.) are given in Table 1. Horizontal dotted gray line mark r = 0, no change in population size.

Figure 4. Simulated population dynamics in the East European vole in Svalbard. (**a**) Bifurcation diagram for autumn densities for increasing fixed amounts of ROS every winter using the population model with no process error ($r_{w,t} = \beta_{w,0} + \beta_{w,X} * X_{w,t} + \beta_{w,ROS} * ROS_t$, parameter estimates in Table 1 but $\sigma^2_{i,r}$ set to zero). (**b**) Bifurcation diagram for the effect of changing the length of the winter season (Δt_w) on autumn densities in the baseline population model with zero rain-on-snow and process error (ROS = 0, σ^2_r = 0). (**c**) Estimates of the second order autocorrelation and (**d**) the amplitude of fluctuations (s-index) in autumn densities in the baseline population model for increasing values of process error variance (σ^2_r) and ROS = 0. In **c** and **d**, the long dashed line represents a model where process error only affects the summer population growth, the short dashed line a model where process error only affects the winter population growth, and the solid line represents a model where process error affects equally winter and summer population growth. Estimates of process error variance in models without a ROS effects were $\bar{\sigma}^2_{w,r}$ = 0.014 and $\bar{\sigma}^2_{s,r}$ = 0.020 for winter and summer, respectively. Estimated second order autocorrelation in the Ridge area in August was 0.02, while the s-index was 0.57.

Figure 5. Demographic structure and density dependence based on sex and body size (i.e. sub-adult vs. adults) of East European voles. Sex ratio displayed as **a** the density of sub-adult males plotted against the density of sub-adult females and as **b** density of adult males plotted against

the density of adult females. In **c**, density-dependence in adult males in summer displayed as estimated monthly population growth rate (from time *t* to *t*+1) in adult males plotted against the density of adult males at time t. Estimates from the early (July-August) and late part of the summer (August – September) are given by closed and open circles, respectively. The full line is the regression line estimated using equations (1-5; β_D = -0.043, CI=[-0.073, -0.009]). Black dotted lines are the 95% C.I. for the regression line and the grey dashed horizontal line represents zero population growth. In **d**, recruitment as measured by the density of sub-adults is plotted against the adult female population density. In **a**, **b** and **d**, the 1:1 dotted lines are drawn for visual reference. Bars gives the 95% confidence intervals of estimated densities (**a**-**d**) and population growth rates (**c**).

631 **Figures**

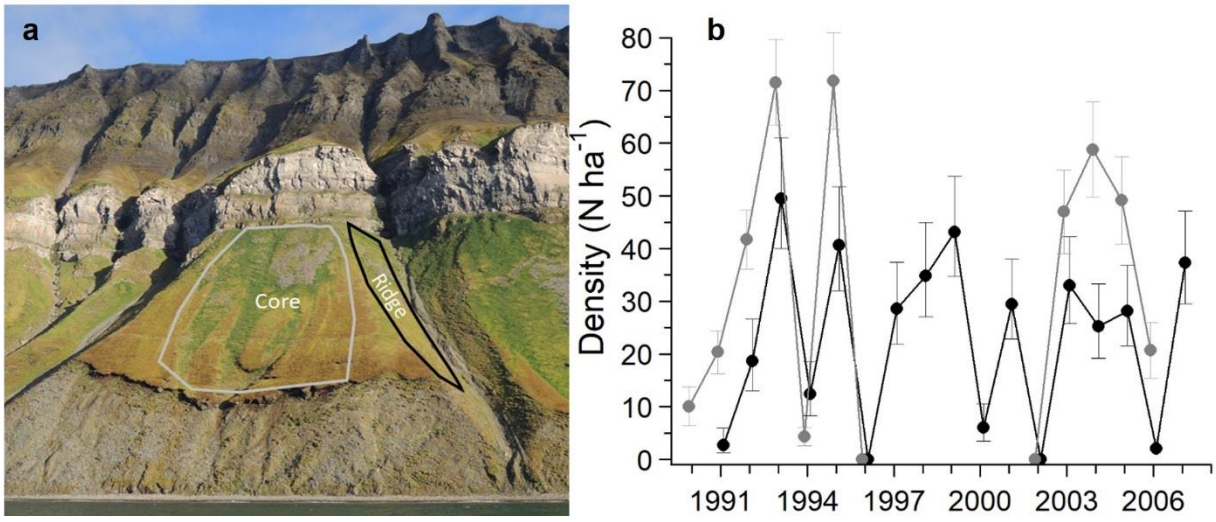

632

633 **Figure 1.**

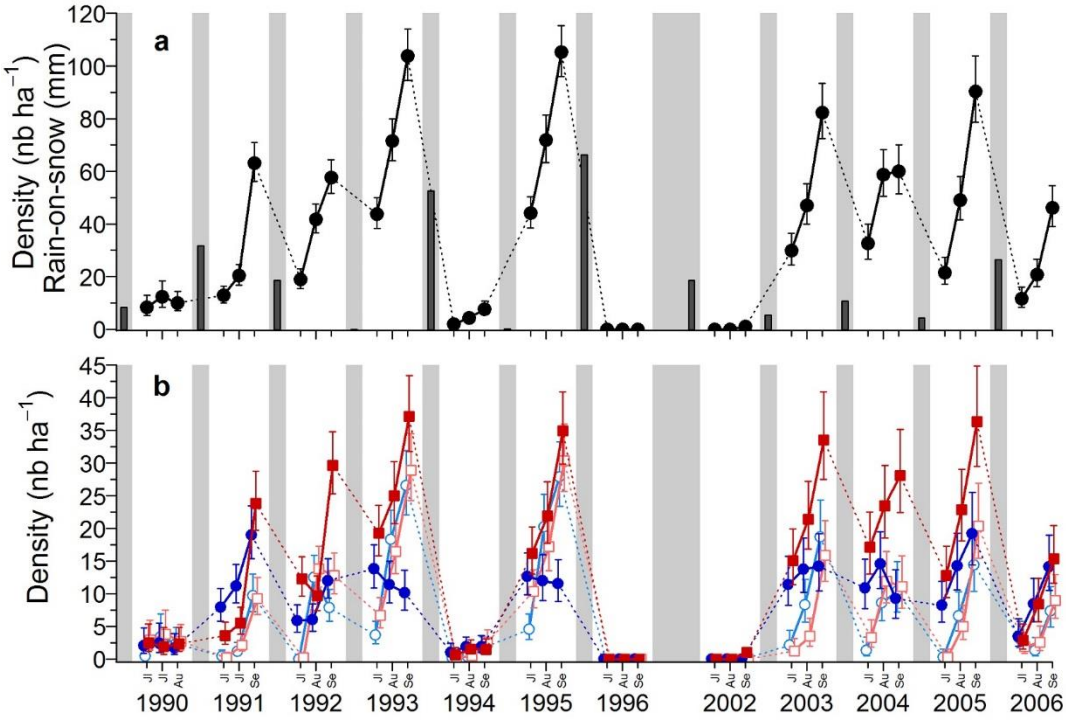

634

635 **Figure 2.**

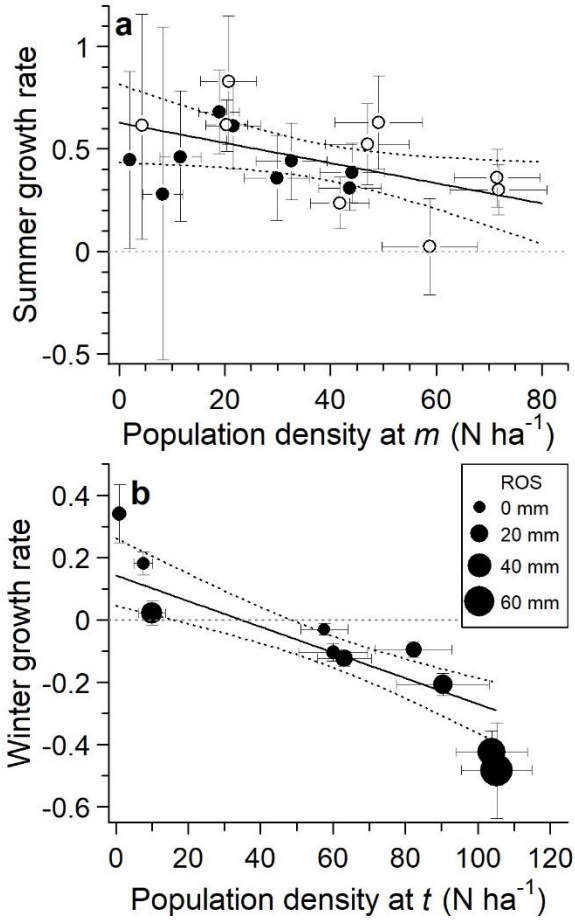

636

637 **Figure 3.**

638

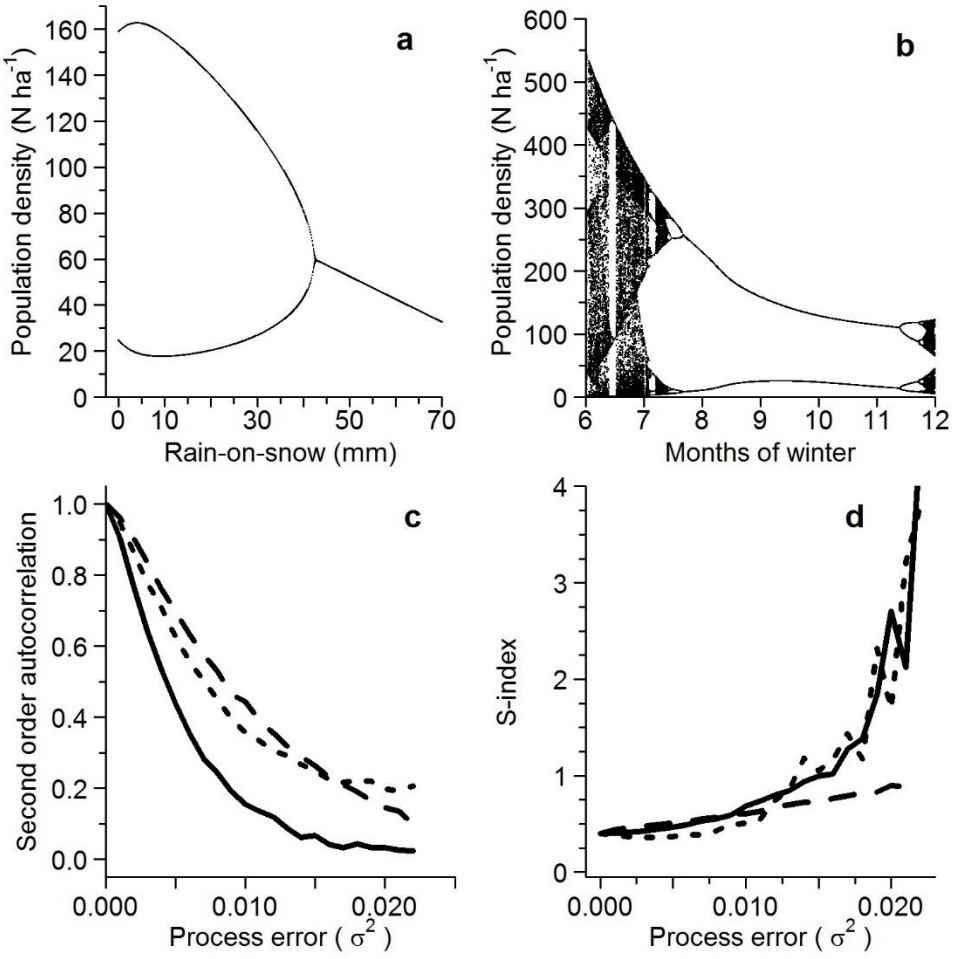
a
Population density (N ha^{-1})
Rain-on-snow (mm)
b
Population density (N ha^{-1})
Months of winter
c
Second order autocorrelation
Process error (σ^2)
d
S-index
Process error (σ^2)

Figure 4.

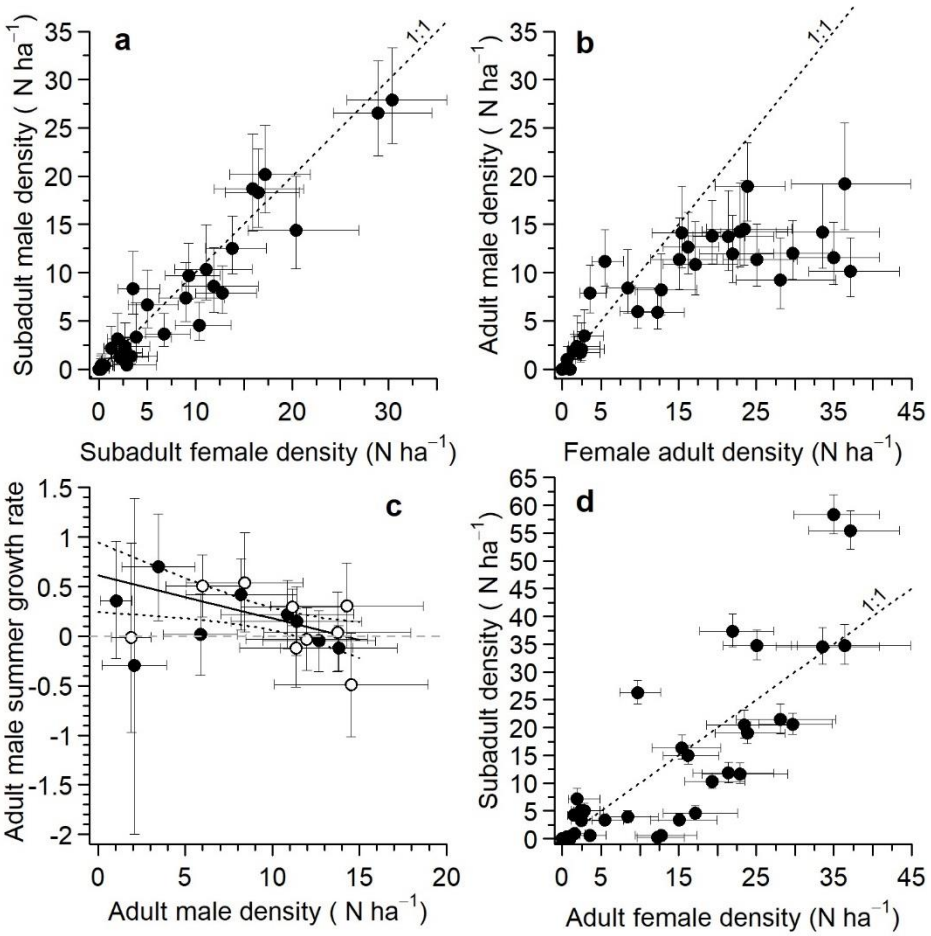

642

643 **Figure 5.**

644 **Supplementary material**

645

646 **Methodological adjustments adopted to handling low and zero population densities when**
647 **estimating of population growth**

648 In September 2002 there were only 3 voles caught and the density was estimated to 1 vole per
649 hectare. However, the mark-recapture analysis did not allow measurement error to be estimated
650 for this density estimate. To overcome this problem with a missing value for the uncertainty
651 associated with the density estimator in subsequent analyses we used the empirical least square
652 linear relationship between $\log(D_t)$ and $\log(\text{var}(D_t))$, $\log(\text{var}(D_t)) = -1.5253 - 0.9479 * \log(D_t)$, to
653 estimate $\sigma^2_{D,t}$ for the last observation in 2002.

654 In June/July 1996, no vole was caught giving an estimate of zero density of voles. No
655 vole was caught in the Core area also in the subsequent trapping periods in 1996, as well as the
656 nearby Ridge area. The most reasonable explanation for the zero observations in 1996 was
657 therefore local extinction in the trapping area, and not that a zero due to measurement error. The
658 previous winter had the highest levels of ROS in the dataset and the population density the
659 previous autumn was also the highest observed, so the handling of the zero observation in 1996
660 could affect estimates of the effect of density dependence and ROS on winter population growth
661 rates. In our estimation of population growth we imputed a small number for the zero
662 observation in June/July 1996. We evaluated the consequence of different choices for the
663 imputed value by fitting the model (equations 1-3) with imputed values for the density in
664 June/July 1996 in the range $\delta = [0.1, 1]$, where 1 vole per hectare is the lowest positive estimate
665 of the density of voles in the study area. Changes in the imputed value mainly affected estimates
666 of the effect of ROS, with increasingly negative estimates of β_C with decreasing δ (point

667 estimates decreasing from -0.0042 to -0.0052). Estimates of β_X (density dependence) were robust
668 to the choice of δ (point estimate range = (-0.0041, -0.0042)). In the results we use δ = 1. This
669 value of δ gave similar parameter estimates to models fitted to data with the observation from
670 June/July 1996 excluded. However, it is noteworthy that more negative effect sizes of ROS are
671 also consistent with the data.
672
673 **Detailed results from the survival and maturation analyses**
674 The data supported a model for survival that included an additive effect of year, and an
675 interaction effect between trapping period, age, and sex (Table S1). Apparent survival rates were
676 highest for adult females (~75-85%/month), whereas sub-adult males had the lowest apparent
677 survival rates (~15-65%/month; Fig. S2). Adult females showed no change in survival rates
678 between the early (July-August) and late (August-September) summer periods. For the other
679 demographic groups of voles survival rates were lower in late summer than early summer
680 (Supplementary material, Fig. S1). This period effect in the survival of males and juvenile
681 females, as well as high survival estimates for the years with very low densities (1990 and 1994),
682 was consistent with density dependent survival density at t and survival between t and $t + 1$ (Fig.
683 S2). The ANODEV confirmed that the survival was negatively affected by density, but this
684 effect was more pronounced in males than females (β = -0.025, 95% CI=[-0.036, -0.013]; Table
685 S2, Fig. S2).
686 Maturation rates varied between years and with an interaction effect between trapping
687 period and sex (Table S1, Fig. S1). We found no significant relationship with density at time t
688 based on the most parsimonious, non-temporal model (β = 0.006, 95% CI: [-0.011: 0.023]; Table
689 S2; Fig. S3). Both sexes had high maturation rates for the July-August period, with males having

690 a 100% maturation probability in all years in this first part of the summer (Fig. S1). Maturation
691 rates were substantially lower in the latter part of the summer (August-September), and males
692 tended to have lower maturation rates than females in this period (Fig. S1).
693
694

Table S1. Ranking of models to test for the effects of time and density on survival (φ) and transition (ψ; maturation) rates of East European voles. The formulae of each model (i) is shown along with its number of parameters (K), ranking parameter $\Delta QAICc_i$, and model weight (w_i). We modelled detection the same way for all models with additive effects of period (t), year, age, and sex. The models that are shown represent those with the highest statistical support ($\Delta QAICc_i < 2$) for the three hypotheses being tested. Time-dependent models shown are those with a $\Delta QAICc_i < 4$ and the one ranked right after. For the density-dependence analyses, we present the models with the highest support without temporal effects and $\Delta QAICc_i$ are calculated based on the top time-dependent model.

	Model			
Type	φ	ψ	K_i	$\Delta QAICc_i$
Time-dependent	year+t.f.sex	year+t.sex	44	0.00
	year+t.sex+f.sex	year+t.sex	42	4.05
Density-dependent survival	D.sex+f.sex	year+t.sex	33	9.87
	D.f.sex+f.sex	year+t.sex	35	10.86
	D+sex	year+t.sex	32	11.22
Density-dependent maturation	year+t.f.sex	D+sex	34	58.54
	year+t.f.sex	D.sex+sex	35	59.08

Note: covariates on detection probabilities were the same for all models and included additive effects of year, primary period, state (subadults, adults), and sex.

t = primary period (July-August, August-September); D = relative density (low, intermediate, high); f = state; + = additive effect; . = interactive effect.

709

710 Table S2. Analysis of deviance (ANODEV) for models without temporal effects to assess

711 density-dependence in survival (φ) and maturation (ψ) of East European voles.

	Model			
Response variable	φ	ψ	*F*-value	*p*-value
Survival	D.sex+f.sex	year+t.sex	3.299	0.043
Maturation	year+t.f.sex	D+sex	6.109	0.018

712 Note: Model comparisons for the ANODEV were based on the full time-dependent model (φ ~

713 year+t.f.sex, ψ ~ year+t.sex, p ~ year+t+f+sex; K = 44) and the simplified model without time or

714 density as a covariate on survival (φ ~ f.sex, ψ ~ year+t.sex, p ~ year+t+f+sex; K = 31) or

715 maturation (φ ~ year+t.f.sex, ψ ~ sex, p ~ year+t+f+sex; K = 33).

716

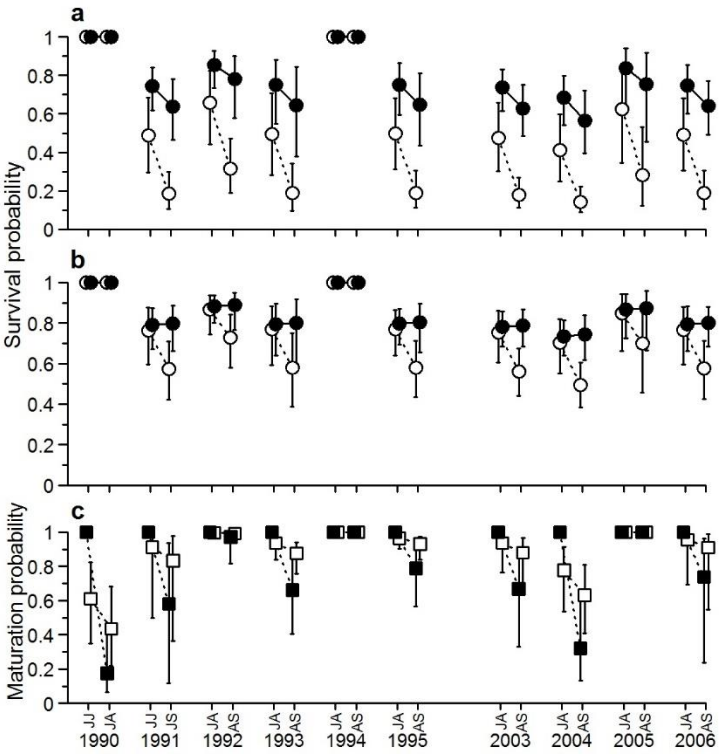

Figure S1. Summer survival estimates of adult (black circles) and sub-adult (white circles) male (**a**) and female (**b**) East European voles and maturation probabilities (**c**) of sub-adult males (white squares) and females (black squares) throughout the years of sampling. Data points are slightly displaced on the x-axis to make confidence intervals more visible. The gap between 1995 and 2003 indicate no data available for summers of 1996-2002 due to sample size being too low or trapping occurred only in August. Error bars are 95% confidence intervals. JJ: early July to late July; JA: late July (1990 only) or mid-July (all other years) to mid-August; JS: late July to mid-September; AS: mid-August to mid-September.

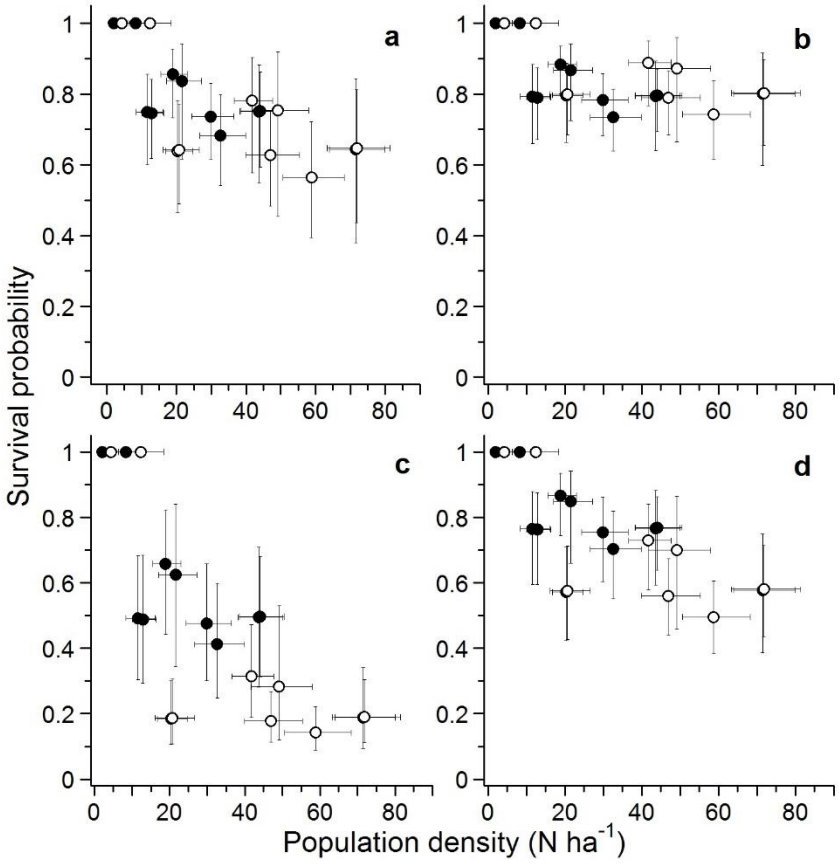

Figure S2. Estimates of survival rates in East European voles between *t* and *t*+1 of adult males (**a**), adult females (**b**), subadult males (**c**), and subadult females (**d**) in relation with population density at *t* from the most parsimonious model (Table S1, time-dependent model $\varphi = f(\text{year+t.f.sex})$). Filled points represent the period of July-August and open points the August-September period, error bars represent 95% confidence intervals.

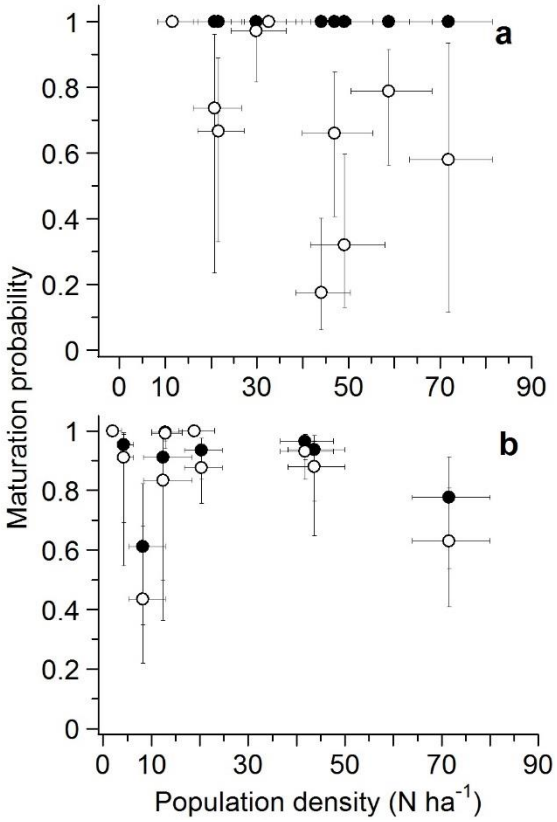

Figure S3. Estimates of maturation rates in East European voles for subadult males (**a**) and females (**b**) from a model with an additive effect of year, and an interaction effect between live-trapping period and sex (ψ = *f(year+t.sex)*, Table 1). Filled points represent the period of July-August and open points the August-September period, error bars represent 95% confidence intervals. Correlation coefficients are given using all the data points (r.all) and excluding the estimates of ψ = 1 (r.sub).